



ELSEVIER

Surface Science 336 (1995) 232–244

surface science

Theoretical study on the chemisorption and the surface reaction of HCOOH on a MgO(001) surface

Hiroshi Nakatsuji^{a,b,*}, Masami Yoshimoto^a, Masahiko Hada^a, Kazunari Domen^c,
Chiaki Hirose^c

^a Department of Synthetic Chemistry and Biological Chemistry, Faculty of Engineering, Kyoto University, Sakyou-ku, 606 Kyoto, Japan

^b Institute of Fundamental Chemistry, Nishihiraki, Sakyo-ku, Kyoto 606, Japan

^c Research Laboratory of Resources Utilization, Tokyo Institute of Technology, 4259 Nagatsuda, Midori-ku, Yokohama 227, Japan

Received 3 January 1995; accepted for publication 27 March 1995

Abstract

The routes and the mechanisms of the molecular and dissociative adsorptions of a formic acid HCOOH and the succeeding migration of a proton on MgO(001) surface are investigated by means of the ab-initio molecular orbital method using the Mg₈O₈ cluster embedded in the electrostatic field due to the 284 point charges on the crystal lattice positions. Both *cis*- and *trans*-formic acids are molecularly adsorbed on an MgO(001) surface with no energy barrier, the *trans* form being more stable than the *cis* form. They are dissociated into a formate anion HCOO⁻ and a proton H⁺ sat on two Mg and O atoms, respectively. We examine the favorable pathway for the dissociation of the O–H bond. The most stable structure of the formate anion is the bridging type on two Mg atoms and the heat of adsorption is 36 kcal/mol. The formate anion adsorbed on the surface activates the surface O atom next to it, because the electrons in the π molecular orbital of the formate anion repel the electrons in the p orbital of this surface O atom, raising it up to the HOMO of the system. The proton adsorbed on the surface O atom hardly migrates because of the high energy barrier of 83–94 kcal/mol, but the existence of the adsorbed formate ion helps this migration by reducing the energy barrier to 44 kcal/mol, through the formation of the molecularly adsorbed formic acid intermediate. The formate anion is shown to be easily tilted on the surface by a small perturbation, leading to an increased interaction between the formate species and the surface.

Keywords: Ab initio quantum chemical methods and calculations; Carboxylic acid; Low index single crystal surfaces; Magnesium oxides; Models of non-equilibrium phenomena; Solid–gas interfaces

1. Introduction

Metal oxide is a good catalyst for a variety of chemical processes as well as a good support for catalysts [1–18]. For example, the decompositions of

methanol [1], ethanol [2,3] and formic acid [4,5] take place easily on the MgO catalyst. In the water gas shift reactions [6–9] on the surface of the metal oxides, like MgO, Al₂O₃ and ZnO, etc., the formate anion is known to be a surface intermediate. However, there are many questions to be solved, such as the nature of the active sites, the structure of the adsorbed species, and the route and the mechanism of the reaction. It has been known that the formic

* Corresponding author.

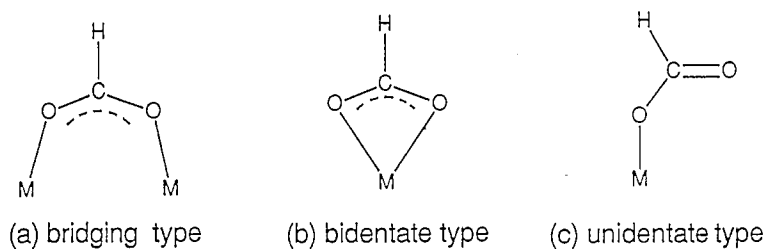


Fig. 1. Three possible geometries of the formate anion on the surface.

acid is adsorbed dissociatively on the metal and the metal oxide surfaces at room temperature and gives formate anion and surface hydroxyl species [4,10–18]. Three types of structures are suggested for the formate anion adsorbed on various metal oxide surfaces [4,10–18]; bridging type, bidentate type, and unidentate type shown in Fig. 1.

The formic acid decomposes on metal and metal oxide surfaces producing $\text{H}_2\text{O} + \text{CO}$ or $\text{H}_2 + \text{CO}_2$ [4,6–18]. Many studies have been done for clarifying the mechanism of the activity and the selectivity of the catalysts in the decomposition reaction of the formic acid. Previously, the dissociative adsorption and the decomposition of the formic acid on the

$\text{MgO}(001)$ single crystal surface are studied by the temperature programmed desorption (TPD) and the sum frequency generation (SFG) methods [4]. The C–H stretching band was observed at 2870 cm^{-1} , and the formate ion on the $\text{MgO}(001)$ surface is assigned to be either the bridging or bidentate type.

Theoretical study for surface reactions can provide information on the active site and the mechanism of the reaction, and many such studies have been reported for the hydrogen chemisorption on an MgO surface [19–21] and other metal oxides surfaces [22–25]. In this paper, we report a theoretical study on the molecular and dissociative adsorptions of the formic acid on the MgO surface and the

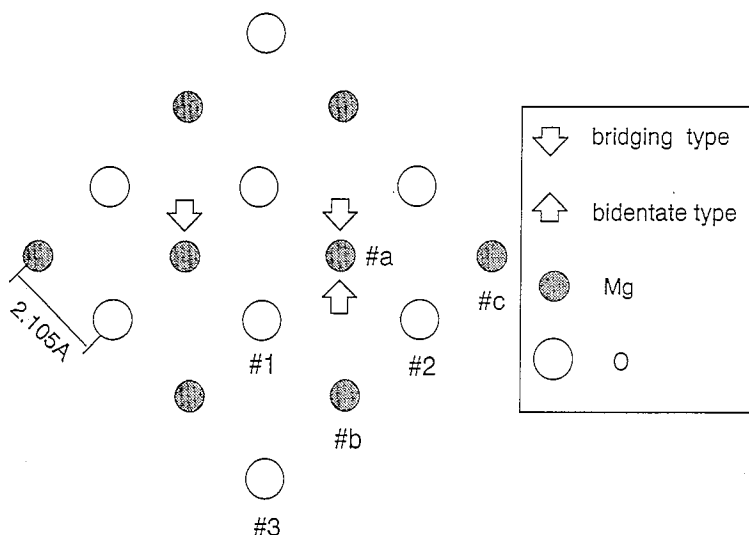


Fig. 2. Mg_8O_8 cluster as a model of the $\text{MgO}(001)$ surface. This cluster is taken from the first layer of the MgO surface and put in the electrostatic field presented by 284 point charges located on the MgO crystal lattice. The central Mg_2O_2 in the cluster is used for the adsorption and dissociation of HCOOH . The arrows indicate the sites of the adsorption of the formate anion in the bridging and bidentate forms.

succeeding proton migration mechanism on the surface.

2. Model and calculational method

The MgO(001) surface is represented by the Mg_8O_8 cluster shown in Fig. 2 embedded in the electrostatic field. The point charges situate at the 284 lattice sites of the first, second and third layers around this Mg_8O_8 cluster. The net charges of the naked Mg_8O_8 cluster are calculated to be 1.3–1.5 for the Mg atoms and -1.5 to -1.3 for the O atoms. We therefore choose the point charges $+1.0$ for the Mg sites and -1.0 for the O sites to prevent the overestimation of the Coulomb interaction between the cluster and the lattice point charges. The cluster geometry was fixed at the crystal lattice position with the MgO distance of 2.105 Å during the surface reaction processes. The relaxation of the MgO surface has been found to be very small [26]. Nevertheless, the surface relaxation effect might be important in the chemisorption and surface reaction processes. However, a large number of the degrees of freedom of the surface implies a formidable optimization problem when it is included in the reaction path calculations. Therefore, in the present study, we did not include the effect of the relaxation of the MgO surface. Only the geometries of the adsorbates are optimized using the energy gradient method.

We investigate the reaction on a clean flat surface. As the reaction site for the adsorption and dissociation of the formic acid, we use the central Mg_2O_2 part of the cluster, since these atoms have adequate neighboring atoms of the first layer. For example, the bridging and bidentate type formic acids are assumed to be adsorbed on the Mg atoms shown by the arrows in Fig. 2.

The basis set used for the Mg atom is the (3s3p)/[2s2p] set of Wadt and Hay [27] and the Ne core is replaced by the effective core potential. For C and O atoms, the (9s5p)/[4s2p] set of Huzinaga and Dunning and for H atom the (4s)/[2p] set are used [28,29].

The calculations are done at the Hartree-Fock and the MP2 levels with the use of the program HONDO7 [30].

3. Molecular adsorption of formic acid on MgO(001) surface

It is known that the formic acid is dissociatively adsorbed on the MgO(001) surface at room temperature [4]. It is also known that the formic acid is molecularly adsorbed on various metal surfaces [15,17]. However, the molecular adsorption of the formic acid on the MgO(001) surface has not been reported. We first investigate the molecular adsorption of the formic acid on the MgO(001) surface.

In a gas phase, the *trans*-formic acid is calculated to be more stable than the *cis* form by 6.4 kcal/mol, and the energy barrier is calculated to be 5.6 kcal/mol relative to the *cis* form. We therefore

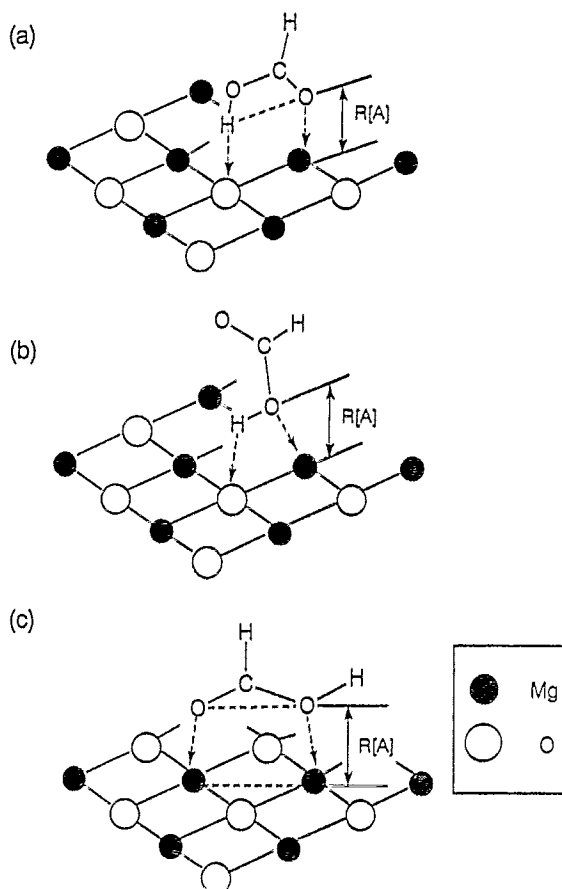


Fig. 3. Assumed path for the molecular adsorption of the formic acid: (a) and (b) *trans*-HCOOH is molecularly adsorbed; (c) *cis*-HCOOH is molecularly adsorbed. R is the distance between the formic acid and the surface.

assume that both *trans* and *cis* forms exist in equilibrium in a gas phase.

We assume the path for the molecular adsorptions of the *cis*-formic acid as shown in Fig. 3c. The two oxygen atoms of the formic acid interact with the two surface Mg atoms, not with the surface oxygen due to the Coulomb repulsion. The molecular plane of the adsorbed formate species on the metal and metal oxide surfaces have been reported to be perpendicular to the surface [5,18,31]. We therefore assume that the molecular plane of the formic acid is perpendicular to the surface. The oxygen–oxygen axis of the formic acid in Fig. 3c is assumed to be parallel to the surface. The optimized geometry is almost the same as in a gas phase as shown in Fig. 4. The adsorption energy defined by the following equation,

$$\Delta E = E(\text{molecular adsorption}) - E(\text{Mg}_8\text{O}_8 \text{ cluster}) - E(\text{cis - formic acid}) \quad (1)$$

is calculated to be 14.3 kcal/mol.

We assume the paths for the molecular adsorptions of the *trans*-formic acid as shown in Figs. 3a

and 3b. The molecular planes of the formic acids are assumed to be perpendicular to the surface. The oxygen–hydrogen axis of the formic acid shown by the broken line in Fig. 3a and the hydroxyl bond of the formic acid in Fig. 3b are assumed to be parallel to the surface. In Fig. 3a, the O and H atoms of the formic acid interact with the surface Mg and O atoms, respectively. In Fig. 3b, the hydroxyl bond interacts with the surface Mg and O atoms. The adsorption energy for the paths (a) and (b) are 14.5 and 8.5 kcal/mol, respectively, showing that the interaction in path (a) is more favorable than that in path (b) because the six-membered surface–molecule local geometry involved in path (a) is more relaxed than the four-membered geometry in path (b). The adsorption energy for the *trans* form defined by,

$$\Delta E = E(\text{molecular adsorption}) - E(\text{Mg}_8\text{O}_8 \text{ cluster}) - E(\text{trans - formic acid}) \quad (2)$$

is calculated to be 20.6 kcal/mol. The geometry of the favorable structure in path (a) is optimized. The geometry is almost same as in a gas phase as shown in Fig. 4.

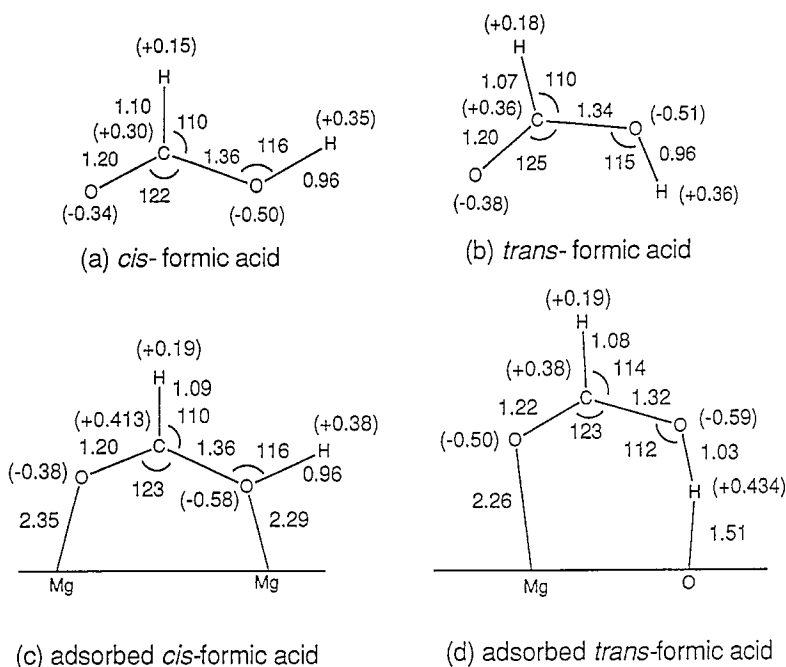


Fig. 4. Fully optimized geometrical parameters of free HCOOH and HCOOH adsorbed on a MgO surface. Bond distances and angles are in Å and degree, respectively: (a) free *cis*-HCOOH; (b) free *trans*-HCOOH; (c) adsorbed *cis*-formic acid; (d) adsorbed *trans*-formic acid. Values in parentheses show the net atomic charge.

The molecular adsorptions of both *trans* and *cis* forms occur with no energy barrier with the adsorption energies of 14 and 21 kcal/mol, respectively. The adsorption energy of the *trans* form is larger than that of the *cis* form. This reflects that the O–H interaction is stronger than the Mg–O interaction. The total net charge on the molecularly adsorbed formic acid shows that the charge transfer, like σ donation or π back-donation, does not occur, but the interaction is essentially electrostatic.

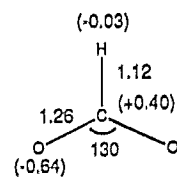
4. Stable adsorption geometry of formate anion on MgO(001) surface

Here we study a stable adsorption geometry and the adsorption energy of the formate anion on the MgO(001) surface. For the former, we examine the bridging, bidentate, and unidentate types shown in Fig. 1. The molecular plane of HCOO^- is assumed to be perpendicular to the MgO plane and stand on the Mg atoms. The unidentate type is not stable on the MgO(001) surface. The optimized geometries of the bridging and bidentate types are shown in Fig. 5 together with those of the free formic acid and the formate anion in a gas phase. The values in parentheses show the Mulliken gross charge.

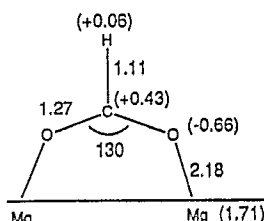
For the free molecules, the geometries of the *cis* and *trans* forms are similar. The OCO angle is larger than 120° , but the COH angle is smaller than 120° . The CO distance of the free formate anion is median between the CO single and double bonds. These characteristics in the geometries are understood from the electrostatic force method [32].

On the MgO surface, the bridging type is calculated to be more stable than the bidentate type: the heat of adsorption is calculated to be 36.0 and 12.0 kcal/mol for the bridging and bidentate types, respectively. Actually the distance between the formate anion and the surface is much shorter in the bridging type than in the bidentate type. The geometry of the formate anion itself does not differ much from that of the free anion. The gross atomic charge is also similar except for the charge of the carbon atom of the bidentate form.

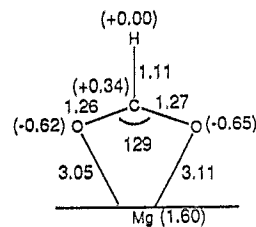
The total charge of HCOO^- is -1.0 , -0.83 , and -0.92 , for the free, bridging type, and bidentate type formate anions, respectively. An electron flow



(a) formate anion



(b) bridging type



(c) bidentate type

Fig. 5. Fully optimized geometrical parameters of free HCOO^- and HCOO^- adsorbed on a MgO surface. Bond distances and angles are in Å and degree, respectively: (a) free HCOO^- ; (b) bridging-type; (c) bidentate type. Values in parentheses show the net atomic charge. The non-symmetry of the bidentate type reflects the non-symmetry of the adsorption site of the cluster shown in Fig. 2.

occurs from the formate anion to the surface and it is largest for the bridging geometry.

Thus, we conclude that the bridging type is the most stable adsorption geometry on the MgO(001) surface; it interacts more strongly with the surface than the unidentate and bidentate types. This result supports the previous result obtained by the SFG experiment [4].

5. Activation of the MgO(001) surface by the adsorbed formate anion

We investigate the effect of the adsorption of the formate anion on the MgO(001) surface by using the Mg_8O_8 cluster shown in Fig. 2. The Mg_8O_8 cluster has three different reaction sites with the different coordination numbers. The surface coordination numbers of the Mg atoms adjacent to the O atoms at the sites #1, #2 and #3 of Fig. 2 are four, three and two, respectively. The coordinatively unsaturated O atoms at site #2 and #3 may be more favorable as a reaction site than the saturated O atoms at site #1. These coordinatively unsaturated sites may be viewed

as representing the kink and step sites on a real MgO surface, while the coordinatively saturated atoms correspond to a flat surface.

We compare in Fig. 6 the MO diagrams of the Mg_8O_8 cluster, the $\text{Mg}_8\text{O}_8 + \text{HCOO}^-$ system, and free formate anion. For the Mg_8O_8 bare cluster, the HOMO consists of the p orbital of the O atom located at the edge (site #3 in Fig. 2) of the cluster. It is vertical to the surface. The p orbital of the O atom at the center of the cluster (site #1 in Fig. 2) is at the lower energy levels as shown by the illustrations in Fig. 6. At the energy levels between HOMO and p orbitals at site #1, there are p orbitals parallel to the surface at site #3. On the other hand, the LUMO is the s orbital of the Mg atom located at #c site, again at the edge of the cluster. The s orbitals of the other Mg atoms constitute the unoccupied MO's next to the LUMO. The unoccupied orbital of the

coordinatively unsaturated Mg atom is at lower energy level than that of the coordinatively saturated Mg atom. The surface coordination numbers of the O atoms adjacent to the Mg atoms at three difference sites, #a, #b and #c are four, three and two, respectively. The order of the energy levels of these unoccupied orbitals is #c < #a < #b. In actual surfaces, these MO levels have some widths and form the band structure.

From the above analysis, the most active site for the electrophile would be the O atom at the edge site #3 of the cluster and for the nucleophile, it is the Mg atom at the edge site #c. The O and Mg atoms on a flat surface (at #1) are less reactive. This result agrees with our experience that the surfaces having some defects are more reactive than a flat surface.

When the Mg_8O_8 cluster adsorbs HCOO^- , the p orbital of the surface O atom at #1, located adjacent

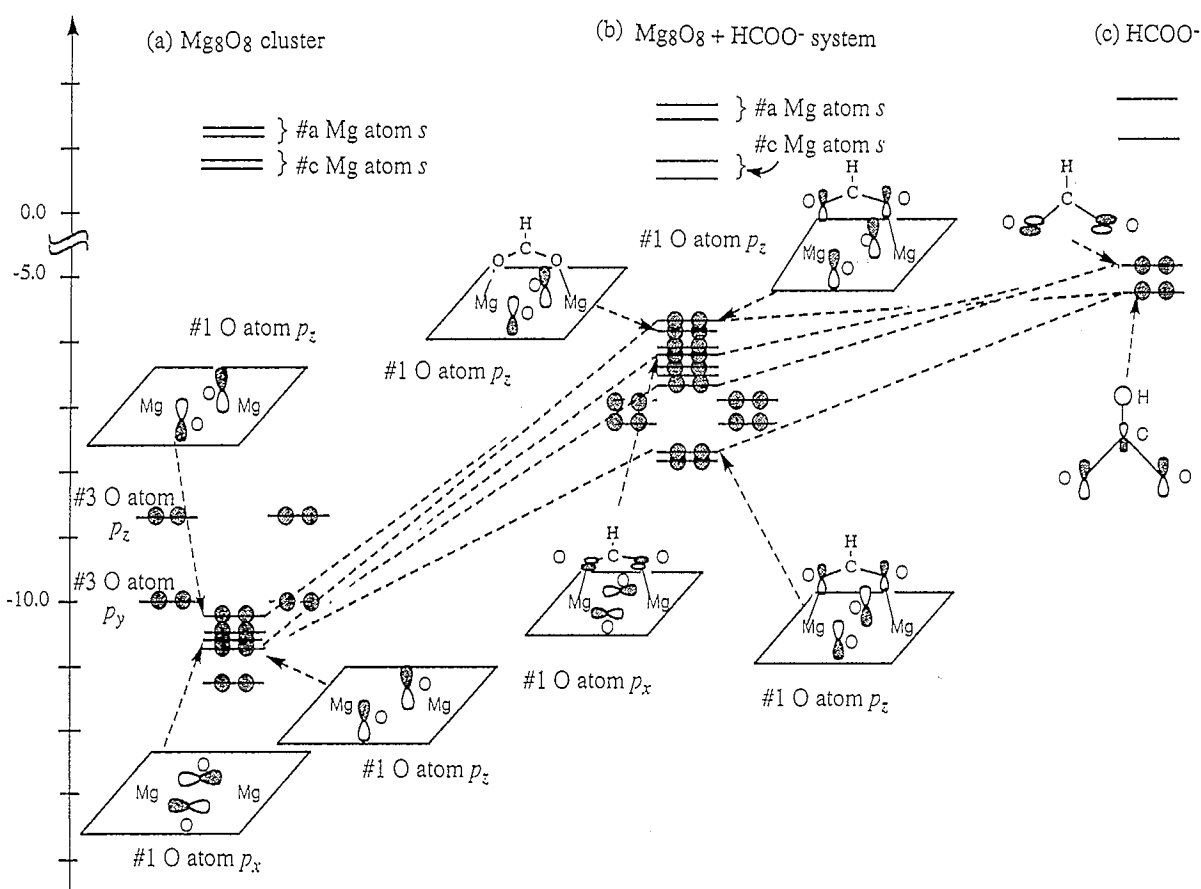


Fig. 6. Schematic molecular orbital diagram for (a) Mg_8O_8 cluster, (b) $\text{Mg}_8\text{O}_8 + \text{HCOO}^-$ system and (c) HCOO^- .

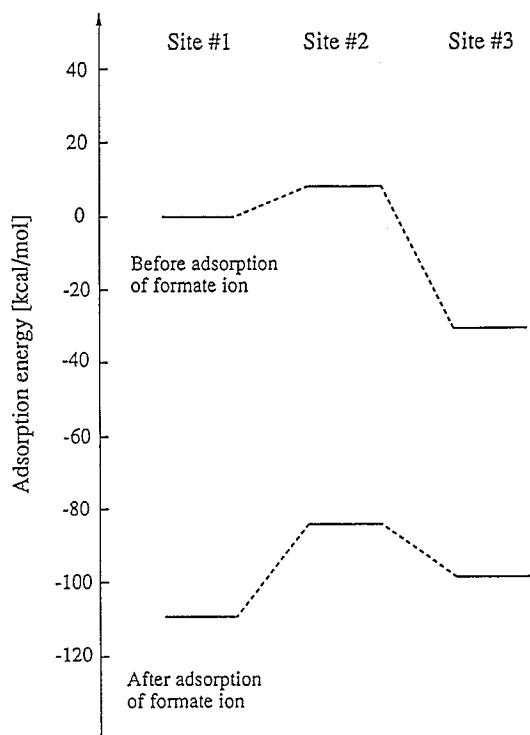


Fig. 7. Relative adsorption energy of proton at site #1, #2 and #3 (defined in Fig. 2) before and after the adsorption of the formate ion. The energy standard is taken for site #1 before adsorption of the formate anion.

to the adsorption site of the formate anion, is activated and moves up to the HOMO, as shown in Fig. 6. The LUMO remains the *s* orbital of the Mg atom at the edge of the cluster and the order of the other unoccupied orbitals also does not change. Thus, when the formate ion is adsorbed, the vertical *p* orbital of the O atom adjacent to the adsorption site of the formate ion is strongly activated for the electrophilic attack.

We investigate the effect of this activation of the surface O atom on the subsequent proton adsorption to the surface. We compare the proton adsorptions to the O atoms at sites #1, #2 and #3 in Fig. 2. The adsorption energy on each site before and after the adsorption of the formate anion is shown in Fig. 7. We assume that the proton is adsorbed at the on-top site and the distance between the surface and the proton is fixed at 0.99 Å, which is the optimized distance for site #1 before the adsorption of the formate ion. The adsorption energy for site #3, located at the edge of cluster, is largest before the

adsorption of the formate anion, while after the adsorption of the formate anion, the adsorption energy for site #1, adjacent to the adsorption site of the formate anion, is largest. This is the result of the activation of the surface O atom due to the adsorption of the formate anion.

We note that the adsorption energy at site #2 is smallest both before and after the adsorption of the formate ion. This inactiveness of the site #2 is worth noticing.

We think this activation of the surface oxygen atom induced by the adsorbed species would affect a variety of the surface reactions. For example, the mechanism of decomposition of the formate species on the surface should differ from that in a gas phase.

6. The route and the mechanism of transformation from molecular to dissociative adsorptions

We next examine the route and the mechanism of the transformation from molecular to dissociative adsorptions of formic acid on the MgO(001) surface. We examine the routes starting from the *cis*- and *trans*-formic acids adsorbed on the surface.

We consider the paths A and B shown in Fig. 8 starting from the *cis*-formic acid. In paths A and B, the hydrogen migrates to site I and site II, respectively, of the surface.

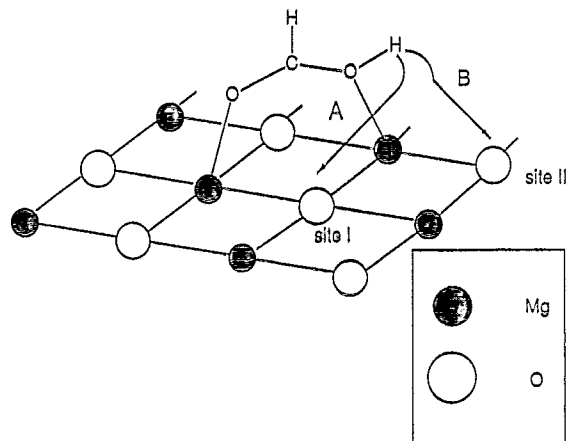


Fig. 8. Dissociation path of the OH bond of the molecularly adsorbed *cis*-HCOOH on the MgO surface. In path A, the H atom migrates from HCOOH to site I on the surface and in path B, it migrates to site II.

In Fig. 9, we show a different view of path A: it is normal to the surface Mg–O (site I) axis. The point #1 corresponds to the molecular adsorption and #5 to the dissociative adsorption. The H atom rotates from #1 to #2 with the OH distance fixed and parallel with the MgO axis. At #3, the H atom lies just at the median of the MgO axis and only the distance between H atom and the surface is optimized to be 1.77 Å. At #5, the H atom lies on top of the surface O at site I and the distance is optimized to be 0.98 Å. At #4, this OH distance is the same, and the distance of H from the MgO axis is optimized to be 0.85 Å. In path B, the H atom migrates just in the same way as in path A, replacing the Mg–O (site I) axis with the Mg–O (site II) axis.

Fig. 10 shows the energy profile for the dissociation from *cis*-formic acid adsorbed on the MgO surface, where ΔE is calculated by,

$$\Delta E = E - E(\text{Mg}_8\text{O}_8 \text{ cluster}) - E(\text{cis-formic acid}). \quad (3)$$

The energy barrier for path A is 34.0 kcal/mol from the molecular adsorption state and the heat of the dissociative adsorption is 20.0 kcal/mol. Path B is less favorable in both the barrier height and the adsorption energy.

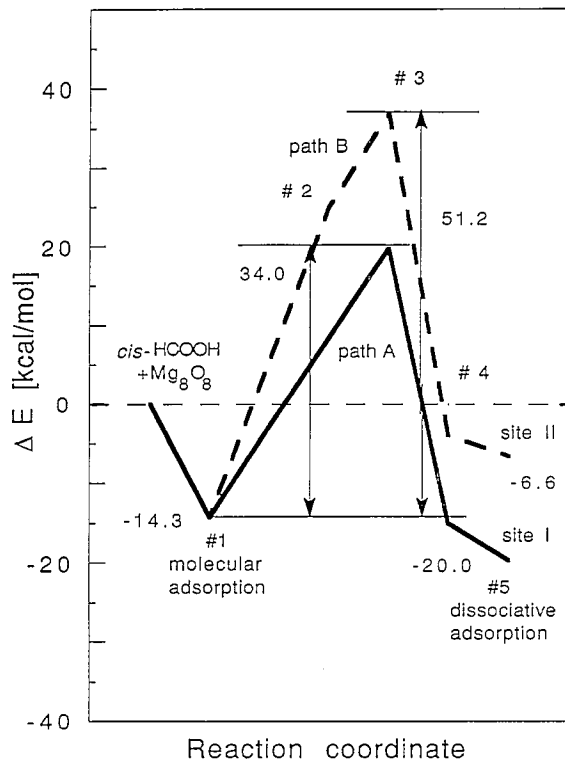


Fig. 10. Energy profile for the dissociation of the molecularly adsorbed *cis*-HCOOH on the MgO surface.

The favorable nature of path A is due to the two reasons. First, in the initial stage of path A the H atom can interact with the $p\pi$ orbital of the formic acid and second in the later stage the H atom is adsorbed at the surface O atom at site I which is activated by the adsorption of the formate anion which is the product of this reaction.

Next, we show in Fig. 11 the assumed pathway of the OH bond cleavage of the molecularly adsorbed *trans*-formic acid. When formic acid is molecularly adsorbed, the interaction between the hydrogen of the formic acid and the surface O atom occurs. This O–H interaction promotes the cleavages of the hydroxyl bond of the formic acid and gives the essentially unidentate formate anion. Because the unidentate configuration is unstable as discussed in Section 4, it is transformed into the bridging form, leaving a proton on the surface O atom.

For studying this O–H bond cleavage process, we fix the geometry of the formate anion and the length between the surface Mg atom and the O atom of the

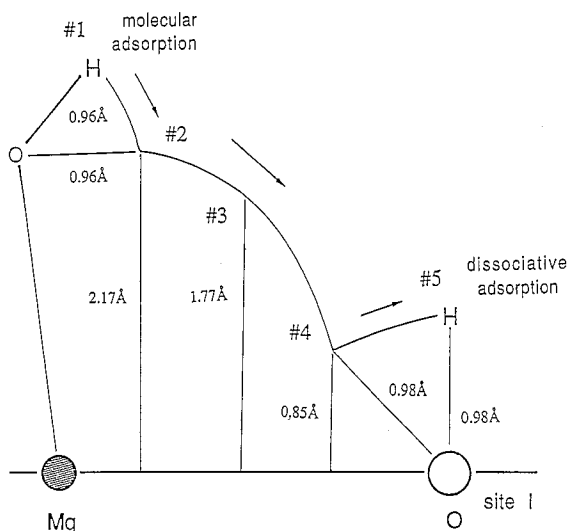


Fig. 9. A sketch of the dissociation path of the OH bond of the *cis*-HCOOH in path A. Only the distance between the proton and the surface is optimized.

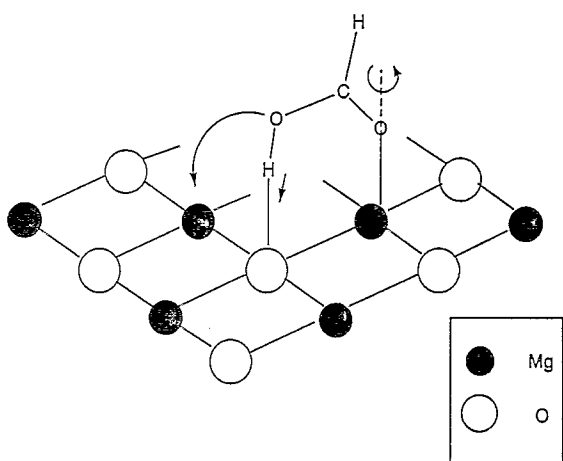


Fig. 11. Dissociation path of the OH bond of the molecularly adsorbed *trans*-HCOOH on the MgO surface.

formic acid. The molecular plane of the formate anion is rotated around this MgO bond to form another MgO bond. We calculate the energy difference ΔE by,

$$\Delta E = E - E(\text{Mg}_8\text{O}_8 \text{ cluster}) - E(\text{trans-formic acid}), \quad (4)$$

and show the energy profile for the above assumed path in Fig. 12.

The energy barrier for the dissociation starting from the *trans* form is calculated 17.4 kcal/mol. It is smaller than that starting from the *cis* form shown in Fig. 10. The interaction between H and the surface O atom facilitates the cleavage of O–H bond. However, in Fig. 12, the dissociatively adsorbed state is

Table 1
Molecular and dissociative adsorption energies and the energy barriers in kcal/mol calculated at the HF and MP2 levels

	<i>cis</i> -formic acid		<i>trans</i> -formic acid	
	HF	MP2	HF	MP2
Molecular adsorption energy ^a	-14.3	-47.9	-20.6	-59.2
Energy barrier for dissociation ^b	34.0	28.7	17.4	12.8
Dissociative adsorption energy ^a	-20.0	-51.7	-13.6	-49.0

^a Relative to the corresponding free formic acid and surface.

^b Relative to the corresponding molecularly adsorbed state.

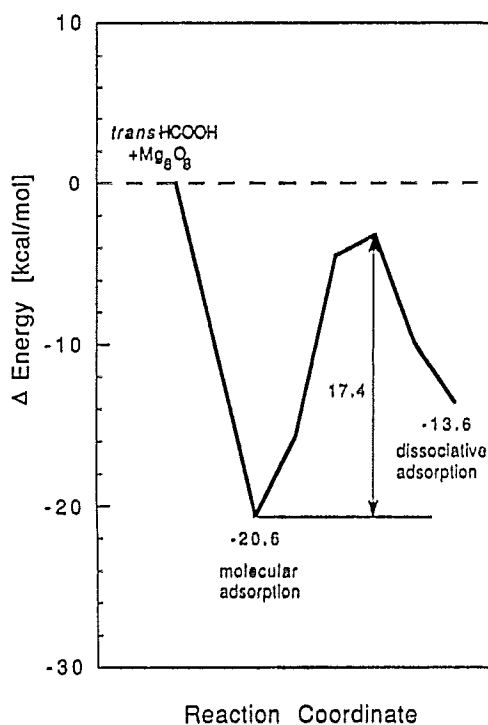


Fig. 12. Energy profile for the dissociation of the molecularly adsorbed *trans*-HCOOH on the MgO surface. Paths (a) and (b) are defined in Fig. 11.

calculated to be less stable than the molecularly adsorbed state, which may not be consistent with the experimental result [4].

We examine the effect of the electron correlation at the MP2 level: we calculate the MP2 energy at the geometry optimized at the HF level and show the results in Table 1. At the MP2 level the adsorption energies are much larger than those at the HF level and the energy barriers for the dissociation are smaller than those of the HF level. The qualitative nature does not change, but at the MP2 level, the geometry should also be optimized at the MP2 level.

7. Migration of proton on the MgO(001) surface

It is known that a proton migrates easily on metal surfaces [33]. We study here the migration of a proton on the MgO(001) surface, which is a metal oxide and is an insulator, and further about the effect of the adsorbed formate ion on the migration of the

proton. We examine several paths shown in Fig. 13 for the migration of a proton on the surface before and after the adsorption of the formate ion. The distance between the proton and the surface is optimized for each path.

In path α of Fig. 13a, a proton moves straight from one O atom to another adjacent one on the surface before the adsorption of the formate ion. The energy barrier is 93.5 kcal/mol and this value is essentially the same as the dissociation energy of the OH bond, i.e., 101 kcal/mol [34]. We next investigate the same path after the adsorption of the formic acid. When a proton migrates from site I to III on the surface as shown in Fig. 13b, the energy barrier is 83.5 kcal/mol. When the proton migrates from site IV to III, the energy barrier is 94.7 kcal/mol. Therefore, the path that the proton moves straight from one O atom to another on the surface is not realistic.

Next, we examine path β shown in Fig. 13a in which the proton first migrates from O to the adjacent Mg atom and then from this Mg to the O atom. The energy barrier is 167.7 kcal/mol: the proton is unstable on the Mg atom because of the similar positive charges. We have also investigated path γ shown in Fig. 13a and found that the order of the energy barrier is

path $\beta > \text{path } \gamma > \text{path } \alpha$.

We next examine the two paths in the existence of the formate anion as shown as path A and B in Fig. 13b. Both paths have two steps and the first step is similar. It is the movement of a proton from the surface O atom to the O atom of the adsorbed formate ion to form the O–H interaction. At the end of the first steps of both paths, the proton is situated at the distorted *cis* form of the molecularly adsorbed

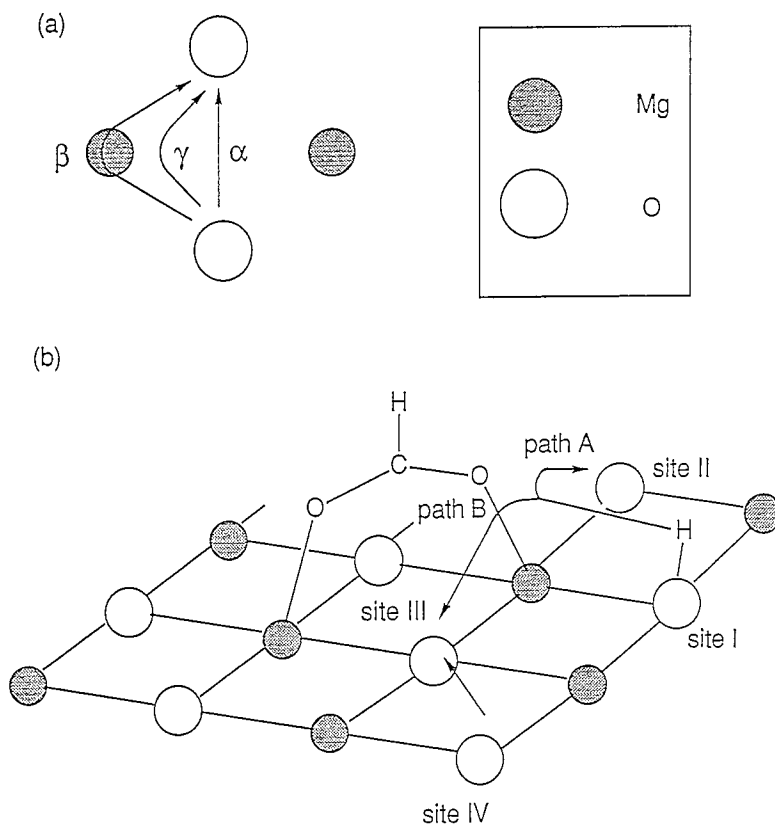


Fig. 13. Proton migration paths on the MgO surface, before and after the adsorption of HCOO^- .

formic acid. The energy is the same for the first step of both paths. The second step is the movement of the proton to another surface O atom as shown in Fig. 13b. In path A, the proton migrates from site I to II, and in path B, the proton migrates from site I to III.

The energy profiles of path A and B are shown in Fig. 14. The energy barrier of the first stage is 43.5 kcal/mol for both paths and the system is stabilized by 7.7 kcal/mol through a formation of the OH bond. The energy barrier for the second stage is 51.2 kcal/mol for path A and 20.5 kcal/mol for path B; the energy barrier in path B is smaller than that in path A. The lower energy barrier in path B is due to the fact that the proton interacts more easily with the HOMO of the formate anion, which is the non-bonding π MO localized on oxygen as shown in the right hand side of Fig. 6. The adsorption energy at site III is larger than that at site II, because site III is just the position activated by the presence of the adsorbed formate anion as discussed in the above section.

Thus, the energy barrier for the proton migration is much smaller when the formate anion exists on the

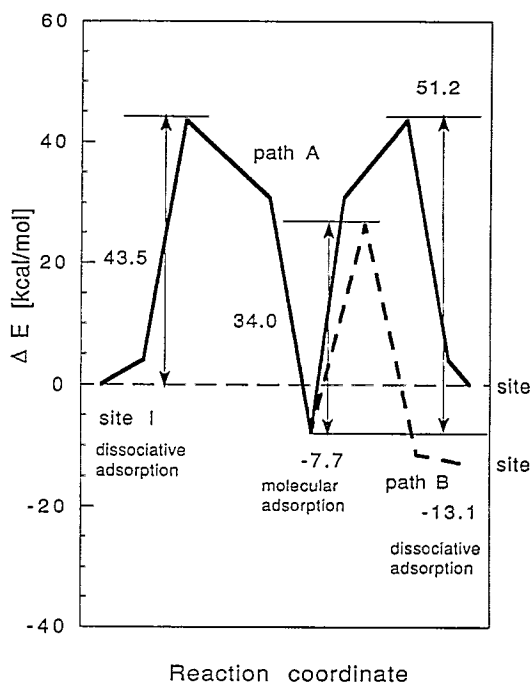


Fig. 14. Energy profile for the migration of a proton. Paths A and B are defined in Fig. 13.

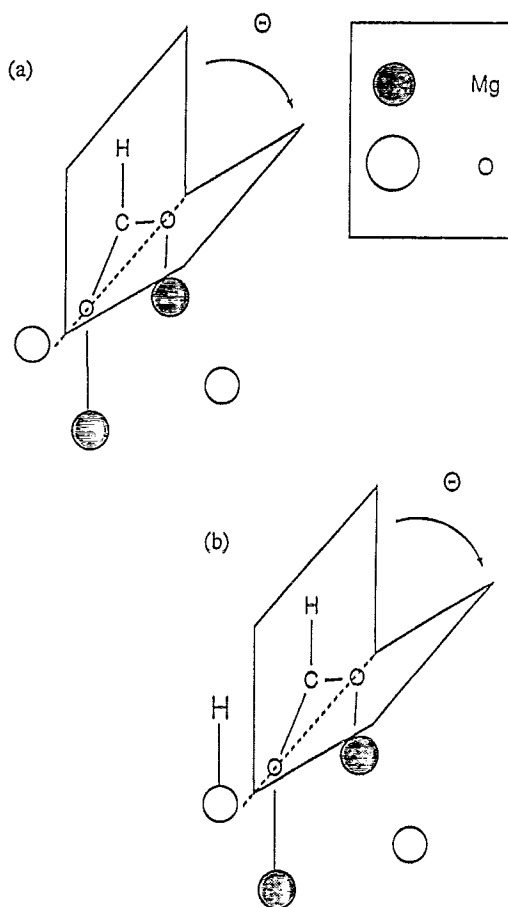


Fig. 15. Tilting of the formic anion on the MgO(001) surface. $\Theta = 0$ denotes the molecular plane vertical to the surface and $\Theta = 90$ the molecular plane parallel to the surface. (a) The system of only the adsorbed formate anion. (b) The system of the adsorbed formate anion and the adsorbed H atom.

surface. This is because the proton migrates not directly but through the formation of the molecularly adsorbed formic acid.

8. Tilting of the molecular plane of the formate ion on MgO(001) surface

We investigate here whether the molecular plane of the formate ion tilts toward the MgO(001) surface, and if so, how much and how easily does it tilt. Fig. 15 shows the tilting of the formate molecular plane on the MgO surface. We use the bridging geometry and the height of two oxygen atoms of the adsorbed

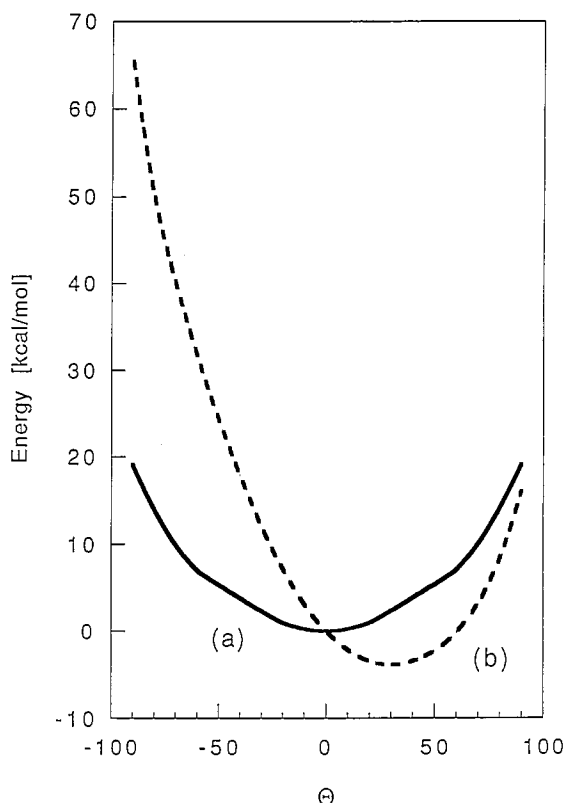


Fig. 16. Potential curve for tilting the adsorbed formate anion on the MgO(001) surface. Solid and broken lines correspond to the cases (a) without and (b) with the proton.

formate anion from the surface is fixed and the geometry of the formate is also fixed. The angle between the molecular plane and the plane vertical to the surface is expressed by the Θ . The formate ions vertical and parallel to the surface are expressed by the $\Theta = 0$ and $\Theta = 90$, respectively. Fig. 15a is the system of only the adsorbed formate anion and Fig. 15b includes further the adsorbed H atom. In Fig. 15b, Θ is negative when the formate anion tilts toward the adsorbed H atom.

The potential curves for Figs. 15a and 15b are shown in Fig. 16. The most stable structure is at $\Theta = 0$ in Fig. 15a, while it is at $\Theta = 30$ in Fig. 15b. The stabilization energy by tilting in Fig. 15b is only 4 kcal/mol, within the thermal energy. Further, the potential curve for the case (a) is very flat, so that the formate anion easily tilts by a secondary perturbation: the perturbation of only 5 kcal/mol can tilt the formate anion by the angle as large as 50° .

The dynamic bending mode, or the wagging mode of the adsorbed formate anion, which is the tilting mode toward the surface was observed on an Ag surface [18].

On the decomposition of the formic acid into $\text{CO} + \text{H}_2\text{O}$ or $\text{CO}_2 + \text{H}_2$ on the surface, the C–O and C–H bond cleavages should occur in the rate-determining step. Since the C–H bond interacts more effectively with the surface by the tilting of the molecular plane, we expect that the wagging mode is important for inducing the C–H bond cleavage.

We are currently investigating the mechanism of the decomposition reaction of the formic acid on the metal oxide surfaces.

9. Summary

We have investigated the reaction route and the mechanism of the molecular and dissociative adsorptions of a formic acid and the succeeding migration of a proton on a MgO(001) surface by means of the ab-initio molecular orbital method. The surface is represented by the Mg_8O_8 cluster embedded in the electrostatic field due to the 248 point charges placed at the lattice positions of the crystal.

We summarize the results as follows. The bridging type formate ion is more stable than the bidentate type on the MgO(001) surface and the unidentate type is unstable. Both the *trans*- and *cis*-formic acids are molecularly adsorbed without energy barrier and are stabilized on the surface by 21 and 14 kcal/mol, respectively. Then, the OH bond of the formic acid is dissociated to give the adsorbed formate anion and the proton is adsorbed on the surface oxygen. The energy barrier for this dissociation is 17 and 34 kcal/mol, respectively, for the *trans*- and the *cis*-formic acids. The electron correlation effect is examined at the MP2 level.

We found that the p orbital of the surface O atom adjacent to the adsorption site of the formate anion is strongly activated by the presence of the adsorbed formate anion. This activation would affect the courses and the barriers of the surface reactions occurring on this surface. The proton migration on the MgO(001) surface can not occur directly but occurs through the formation of the molecularly

adsorbed formic acid as an intermediate, and in this case the barrier is about 43 kcal/mol. The formate anion easily tilts on the surface, leading to a larger interaction between the formate species and the surface.

Acknowledgements

The calculations have partially been carried out the HITAC M-680H computer at the computer center of the Institute for Molecular Science. The authors thank the IMS computer center for the grant of computing time.

References

- [1] D.C. Foyt and J.M. White, *J. Catal.* 47 (1977) 260.
- [2] (a) S.H.C. Liang and I.D. Gay, *J. Catal.* 101 (1986) 193; (b) N. Takezawa, C. Hanamaki and H. Kobayashi, *J. Catal.* 38 (1975) 101.
- [3] R.O. Kagel and R.G. Greenler, *J. Chem. Phys.* 49 (1968) 1638.
- [4] K. Domen, N. Akamatsu, H. Yamamoto, A. Wada and C. Hirose, *Surf. Sci.* 283 (1993) 468.
- [5] H. Yamamoto, N. Akamatsu, A. Wada, K. Domen and C. Hirose, *J. Electron Spectrosc. Relat. Phenom.* 64/65 (1993) 507.
- [6] T. Shido, K. Asakura and Y. Iwasawa, *J. Catal.* 122 (1990) 55.
- [7] P.J. Meschter and H. Grabke, *J. Met. Trans.* 10B (1979) 323.
- [8] S. Sato and J.M. White, *J. Am. Chem. Soc.* 102 (1980) 7209.
- [9] A. Ueno, T. Onishi and K. Tamaru, *Trans. Faraday Soc.* 67 (1971) 3585.
- [10] Y. Noto, K. Fukuda, T. Ohnishi and K. Tamaru, *Trans. Faraday Soc.* 63 (1967) 3081.
- [11] S. Tanaka, M. Onchi and M. Nishijima, *J. Chem. Phys.* 91 (1989) 2712.
- [12] H. Ohnishi, C. Egawa, T. Aruga and Y. Iwasawa, *Surf. Sci.* 191 (1987) 479.
- [13] S.L. Parrott, J.M. Rogers, Jr. and J.M. White, *Appl. Surf. Sci.* 1 (1978) 443.
- [14] M. Bowker, H. Houghton and K.C. Waugh, *J. Chem. Faraday Trans.* 77 (1981) 3023.
- [15] Y.K. Sun and W.H. Weiberg, *J. Chem. Phys.* 94 (1991) 4587.
- [16] F. Solymosi, J. Kiss and I. Kovacs, *Surf. Sci.* 192 (1987) 47.
- [17] J.L. Falconer and R.J. Madix, *Surf. Sci.* 46 (1974) 473.
- [18] P.A. Stevens, R.J. Madix and J. Stohr, *Surf. Sci.* 230 (1990) 1.
- [19] (a) K. Sawabe, N. Koga and K. Morokuma, *J. Chem. Phys.* 97 (1992) 6871. (b) J.L. Anchell, K. Morokuma and A.C. Hess, *J. Chem. Phys.* 99 (1993) 6004.
- [20] H. Kobayashi, M. Yamaguchi and T. Ito, *J. Phys. Chem.* 94 (1990) 7206.
- [21] E.A. Colbourn and W.C. Mackrogt, *Surf. Sci.* 117 (1992) 571.
- [22] H. Nakatsuji and Y. Fukunishi, *Int. J. Quantum Chem.* 42 (1992) 1101.
- [23] H. Nakatsuji, M. Hada, K. Nagata, H. Ogawa and K. Domen, *J. Phys. Chem.* 98 (1994) 11840.
- [24] (a) H. Nakatsuji and M. Hada, *J. Am. Chem. Soc.* 107 (1985) 8264. (b) H. Nakatsuji, M. Hada and T. Yonezawa, *J. Am. Chem. Soc.* 109 (1987) 1902.
- [25] H. Nakatsuji, Y. Matsuzaki and T. Yonezawa, *J. Chem. Phys.* 88 (1988) 5759.
- [26] S.A. Pope, M.F. Guest, I.H. Hiller, E.A. Colbourn, W.C. Mackrodt and J. Kendrick, *Phys. Rev. B* 28 (1983) 2191.
- [27] W.R. Wadt and P.J. Hay, *J. Chem. Phys.* 82 (1985) 2841.
- [28] S. Huzinaga, *J. Chem. Phys.* 42 (1965) 1293.
- [29] T.H. Dunning, Jr., *J. Chem. Phys.* 53 (1970) 2823.
- [30] H.F. King, M. Dupis, H. Villar and G.J.B. Hurst, Program Library HONDO7 (No. 1501), The Computer Center of Institute for Molecular Science, Okazaki, Japan, 1989.
- [31] M.D. Weisel, J.G. Chen, F.M. Hoffman, Y.K. Sun and W.H. Weiberg, *J. Chem. Phys.* 97 (1992) 9396.
- [32] (a) H. Nakatsuji, *J. Am. Chem. Soc.* 95 (1973) 345, 354, 2083; (b) H. Nakatsuji and T. Koga, in: *The Force Concept in Chemistry*, B.M. Deb (Van Nostrand-Reinhold, New York, 1981) ch. 3, pp. 137-217.
- [33] F.A. Lewis, *The Palladium-Hydrogen System* (Academic Press, New York, 1967).
- [34] C. Calone and F.W. Dalby, *Can. J. Phys.* 47 (1967) 1945.